Proceedings of the 27th International Conference on Automation & Computing, University of the West of England, Bristol, UK, 1-3 September 2022

Data-driven Process Parameter Optimisation for Laser Wire Metal Additive Manufacturing

Matthew Roberts, Min Xia, Andrew Kennedy
Engineering Department, Lancaster University
Lancaster UK
m.roberts7@lancaster.ac.uk m.xia3@lancaster.ac.uk a.kennedy3@lancaster.ac.uk

***Abstract* – Laser Wire Additive manufacturing (LWAM) requires a clear understanding of process parameters and their effects on the geometry and wider material properties of the parts produced to support the production of consistent, repeatable quality parts. Furthermore, its ability to capitalise on using novel alloys depends on efficient characterisation of optimum process parameters. In this work, a method for identifying the range of usable parameters is presented, which produces sufficient data to train Cascade Forward Neural Networks, which are capable of predicting process windows and basic LWAM track geometries for 316L stainless steel. The performance of these networks provides the foundation for further work to identify optimum process parameters and, through transfer learning, may reduce the experimental requirements for the process development of other alloys.**

Keywords-Additive manufacturing; Laser Wire Metal Additive Manufacturing;Directed energy deposition;Machine Learning

I. BACKGROUND

Laser Wire Metal Additive Manufacturing (LWAM or LWMAM) is a subset of the group of metal additive manufacturing technologies known as Direct Energy Deposition (DED) [1]. All of which use an energy source to create a melt pool, delivering metal powder or wire feedstock into it to create a metal bead. These beads or 'tracks' are built up in layers to create cladding on existing metal parts or to form new, fully dense parts which are net shape or near net shape. Fig. 1 shows a simple schematic of the LWAM process where wire of diameter, *d* is fed at speed *u*, into a laser beam of diameter *D* and power, *P*, moving at speed, *v* to create a track of height, *h*, and width, *w*.

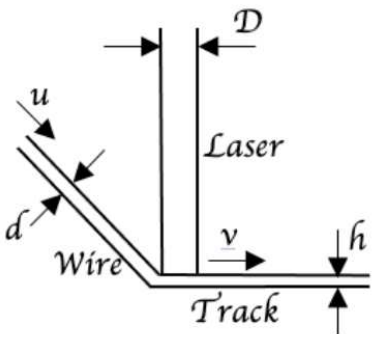

Figure 1 - Schematic of the LWAM process

LWAM is a growing technology area, particularly given the scale and complexity of the parts that are possible, whilst being cleaner and safer than powder-based equivalents. LWAM is also more energy efficient than other wire based DED processes which use other energy sources (for example wire arc or plasma). LWAM can also manufacture parts out of alloys that are not usable in conventional manufacturing processes due to the higher temperatures achieved in the melt pool. However, significant challenges remain for the technology, particularly that of consistency of the quality of repeat parts and between machines, and the reliance on trial and error to refine the process window for each individual part [2-4]. These challenges are broadly a result of the LWAM process being sensitive to variables such as laser configuration, shield gas type and flow, material type, geometry of the part and the thermal field established during the manufacturing process.

Key to addressing these challenges is developing robust methods for structured parameter optimisation, planning and control to ensure the repeatable fabrication of defect-free parts with desirable microstructures and mechanical behaviour. The methods must be themselves repeatable and transferable between alloys and processes, capitalising on the data gathered to reduce the time needed to deliver this and to support qualification of the part and process.

AM Process optimisation is a systematic, numerical characterisation of the process and the subsequent identification of the optimum machine configuration and process parameters to achieve particular targets. Optimal process parameters throughout the printing process are fundamental to a high-quality part and the effects of varying these parameters can be most easily seen in the deposition of simple tracks. Multiple parameters and the resulting geometric and physical properties must be considered to fully optimise a process. To address the complex interactions between parameters and properties Machine Learning (ML) tools are increasingly being used in metal AM research[3].

ML is valuable in AM because of its ability to process non-linear problems, it can cope well with outlying data, it is computationally fast, once trained, and has the ability to understand complex problems without the need for accurate calibration of input parameters[3, 5, 6]. Shallow Artificial Neural Networks (ANNs), such as Cascade Forward Neural Networks, are particularly suited to the

This work is financially supported by the European Regional Development Fund through the Greater Innovation for Smart Materials Optimisation (GISMO) Project (grant reference number 03R18P02671).

non-linear relationships between process parameters and resulting properties. A multi-layer network can learn any finite input-output relationship arbitrarily well, given enough hidden neurons [7].

A significant limitation of ML within the AM field is the relatively small datasets available to train ML models. There are a number of mitigations to this, such as combining experimental data with data from numerical modelling tools [6], using models to generate training data, transfer learning [8] and data augmentation [9]. Despite this, relatively simple shallow ANNs have shown reliable predictions for the distortion of simple parts [5], material properties [10] and thermal modelling [6].

This paper intends to build upon the current understanding and use ML techniques to develop a framework for optimising process parameters for creating single track geometries using LWAM technology. The approach focusses on specific target outcomes for the track geometry so as to build a foundation for improving process optimisation and control in more complex multi-layer builds.

II. EXPERIMENTAL METHODS

The experiments were conducted using a Meltio M450 laser metal wire printer, which uses six laser diodes with a wavelength of 976nm, fed via fibre optics to collimators mounted coaxially around the deposition head. The desired laser power is spread equally between the lasers, giving the system a maximum power of 1200W, Fig. 2 shows the side profile of the print head configuration.

The deposition head remains fixed and the print bed, with substrate attached, moves in the x, y and z plane below. Argon shielding gas is fed locally to the melt pool from the deposition head at a rate of 5.5 litres per minute. The system was configured to use 1 mm diameter 316L stainless steel wire, building onto 15 mm thick 316L stainless steel substrates mounted to the print bed, which is cooled to 13°C. 50mm long tracks were printed 5mm apart, deposited in a random order across the plate, with a three-minute pause between depositions to minimise the effects of substrate heating on the resulting track geometries. This ensured substrate temperature was below 40°C, thereby enabling a fair comparison throughout the trial.

Optimisation studies involved analysing the effect of changes in the laser power *P*, the laser head speed, *v*, and the wire extrusion rate, *u*, on the resultant track geometry of single-track builds. The investigation comprised two steps, the first a broad assessment of the ability to produce tracks of an acceptable geometry (as determined by visual inspection – acceptable being defined as a track that could be selected for using in a part build with a consistent visually smooth top and profile and clean, straight edges securely bonded to the substrate), the second a more refined appraisal of the influence of process parameters on the track geometry for "Good" tracks.

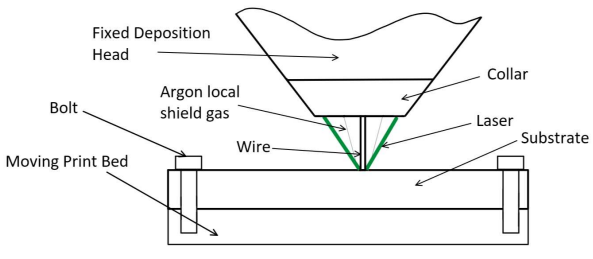

Figure 2 - Schematic of the Meltio print configuration

For the broad assessment, the power was varied from 550 to 950W in increments of 100W, the laser speed from 5 mm/s to 35 mm/s and the wire extrusion rates from 5 mm/s to 55 mm/s. In order to avoid an excessive number of failed prints, on the basis of recommendation of [11], the Wire Speed Factor (WSF - the ratio of the wire to laser speed) was limited to values greater than two. In total, 246 tracks were printed in this first section of the investigation, with approximately 5% of the tracks repeated five times.

From the first set of experiments, the upper and lower bounds for head and extrusion speed were determined for each power level. From this, a Multi-Level Factorial Design of Experiment (DOE) method was used to design the second set of experiments using Minitab statistical software. General full factorial designs were created for the same powers as the previous experiment and within the limits of speeds identified, the design used two factors, laser and extrusion speed for each power, with three or four levels depending on the range of parameters evaluated, 151 tracks were produced. Of these tracks, 37 were deemed good and were reprinted on 3mm thick 316L plates overlaying the 15mm substrate. This was performed not just to ensure repeatability, but in order to permit the tracks to be placed on the bed of an Olympus LEXT OLS5100 Laser Microscope so that the geometry of the tracks could be measured.

Measurements with the laser microscope were taken at five places across the length of each track, 10mm at each end of each track was omitted to avoid skewing the measurements by the effects of the 'laser switch on' and 'laser switch off' process of the machine. Track height and width was measured and the standard deviation of these calculated to indicate consistency. Fig. 3 shows the typical track height and width geometry measured by the microscope. Measurements were filtered using a traveling average filter to remove noise from the measurement process.

Measurement data for the geometry of the track were used, along with input process data, to train ANN models. MATLAB r2020a was used to create the models in the

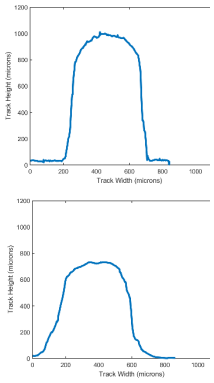

Figure 3 - Typical geometries for the tracks as measured by the laser microscope

study and Cascade Forward Neural Networks were selected after a comparison of the performance of a number of different neural network architectures. The networks were repeatedly trained in loops of 200 cycles with different configurations of layers and node numbers to find the highest R ratio and the lowest Mean Square Error (MSE). It was found that two hidden layers were most effective, with 20 nodes in the first and 14 in the second. Fig. 4 shows the configuration of the network. The default transfer functions for the hidden layers were used, Hyperbolic Tangent Sigmoid for the first and Linear for the second. The training function used was Levenberg–Marquardt and the performance function was MSE. 70% of the data were randomly selected to train the networks, 15% were used for verification, and 15% for testing.

Two sets of Cascade Forward Neural Networks were trained, the first to predict whether the track would be successful, based on the track quality assessment, the second to predict track geometry. Both networks used the input parameters of power, head speed, extrusion rate and WSF. The first network had the track quality as the response, which was represented as a value between 0 and 1, which was interpreted as a confidence level, where values above 0.8 were considered 'Good'. The second used the measured track geometry information, which included track width, height standard deviation of width and height along its length (to indicate consistency and 'waviness' of the track) and the height to width ratio.

III. Results and Analysis

An image of a plate with deposited tracks is shown in Fig. 5. Across all of the experiments, a small proportion of the tracks (4%) were classified differently on their repeat going from 'Good' to fail or vice versa, resulting in some parameter combinations appearing ambiguous as to whether they could produce successful tracks. There were however clear windows where combinations of parameters were identified that produced consistently good quality tracks. These process windows are plotted in Fig. 6, for powers of 550W, 750W and 950W.

Measurement data for the 37 "good" tracks, used in the second ANN, are shown in Table 1. Broad trends in these data can be observed. At a given power and extrusion rate, as the laser head speed increases, the width and height of the track both tend to decrease. Similarly, for a fixed laser head speed, as the extrusion rate increases, so do both the track height and width. These relationships are expected from the conservation of material deposited. When the head speed and extrusion rate are fixed and the power increased, the track height decreases and the width tends to increase. For all these cases the effect on the track height is much clearer than on the width. All these trends agree with observations in the literature [12, 13].

Image a. in Fig. 7 shows a successful track within the process window, for a laser power of 950W. Outside of the process window, different types of defective tracks can be identified. As the head speed increases, for the same extrusion rate, (image b) the track cross sectional area must decrease, and reduced substrate melting prevents

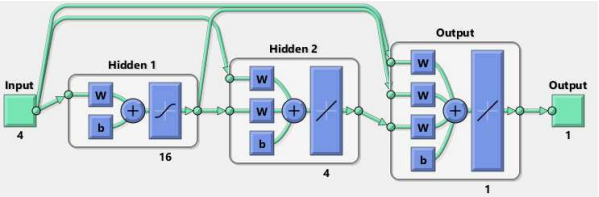

Figure 4 - Schematic of the configuration of the ANN

Figure 5 - Examples of deposited tracks

TABLE I. Process and Geometry Data for "Good" Tracks

Power	Laser Speed	Extrusion Rate	WSF	Width (mm)	SD of Width	Height (mm)	SD of Height	H-W Ratio
550	3.75	15	4.00	3.09	0.62	1.85	0.04	0.63
550	5	15	3.00	1.75	0.01	1.59	0.01	0.91
550	6	15	2.50	2.77	0.56	1.38	0.02	0.52
550	7.5	15	2.00	1.56	0.02	1.21	0.02	0.77
550	9.25	16	1.73	1.49	0.03	1.10	0.02	0.74
550	10	15	1.50	1.61	0.06	0.92	0.02	0.57
550	10	20	2.00	1.46	0.20	1.23	0.07	0.86
650	8.7	17.4	2.00	1.56	0.06	1.18	0.02	0.76
650	10	18.75	1.88	1.66	0.06	1.07	0.02	0.65
650	16	18.75	1.17	1.69	0.05	0.74	0.01	0.43
750	5	20	4.00	3.25	1.03	1.76	0.02	0.59
750	5.1	20.4	4.00	3.27	0.13	1.77	0.02	0.54
750	5.83	20.4	3.50	2.09	0.03	1.59	0.01	0.76
750	6.8	20.4	3.00	2.02	0.05	1.41	0.02	0.70
750	8.16	20.4	2.50	2.01	0.04	1.23	0.02	0.61
750	10	20	2.00	1.80	0.06	1.09	0.01	0.60
750	10.2	20.4	2.00	1.87	0.03	1.02	0.01	0.54
750	13.6	27.2	2.00	1.73	0.08	1.09	0.04	0.63
750	17	34	2.00	1.67	0.04	0.95	0.05	0.57
750	18.7	37.4	2.00	1.62	0.07	0.97	0.02	0.60
850	10	26.7	2.67	2.00	0.06	1.29	0.02	0.64
850	11.4	22.8	2.00	1.84	0.05	1.05	0.02	0.57
850	15	26.7	1.78	1.94	0.03	0.95	0.02	0.49
850	15.2	30.4	2.00	1.78	0.09	1.01	0.06	0.57
850	19	38	2.00	1.68	0.06	1.05	0.06	0.62
850	20.9	41.8	2.00	1.69	0.03	0.94	0.07	0.55
850	22	26.7	1.21	1.80	0.06	0.71	0.02	0.39
850	25	27	1.08	1.65	0.07	0.68	0.03	0.41
950	6.45	25.8	4.00	2.31	0.06	1.69	0.03	0.73
950	7.37	25.8	3.50	3.14	0.53	1.52	0.01	0.50
950	8.6	25.8	3.00	2.19	0.08	1.38	0.01	0.63
950	10.32	25.8	2.50	1.98	0.05	1.20	0.01	0.61
950	12.9	25.8	2.00	1.93	0.03	1.00	0.02	0.52
950	17.2	25.8	1.50	1.78	0.05	0.84	0.01	0.47
950	17.2	34.4	2.00	1.76	0.08	1.07	0.04	0.61
950	21.5	43	2.00	1.66	0.08	0.95	0.04	0.57
950	23.65	47.3	2.00	1.66	0.04	0.94	0.02	0.57

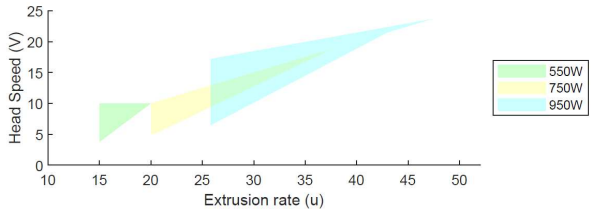

Figure 6 - Schematic of the process window for "Good" tracks

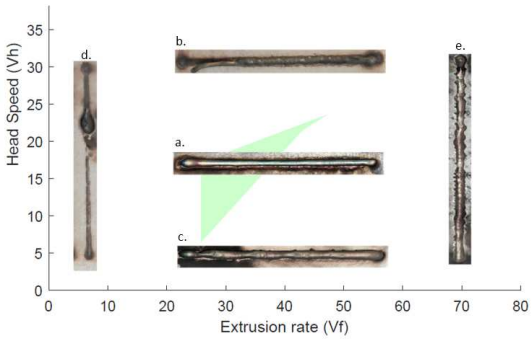

Figure 7 - Process window and track geometry for 950W

good bonding. Conversely as the head speed slows, (image c) the track cross section increases and unstable wavy tracks are formed from the excessive material in the melt pool. At a given laser head speed, when the extrusion rate is too slow, (image d) the energy input per unit volume of material is too high and the wire melts before it reaches the substrate, creating intermittent balls of melted material. When the extrusion rate is too high (image e) there is insufficient energy to melt the high throughput of material.

Predictions for geometry and track success were made using the test data and the two Cascade Forward Neural Networks designed for geometry and quality. To address the relatively small number of training data, particularly for track geometry, data augmentation was used to improve the network training, whereby the data was used twice by appending it in reverse order to the training data set. This resulted in 74 response variables for track geometry training, validation and testing. All tracks printed throughout the experimental process were evaluated as 'Good' or 'Failed', resulting in 511 responses, with augmentation this provided 1022 response variables for track quality.

Track quality predictions resulted in track success being accurately predicted in 98% of cases. Albeit random, most of the test data was likely within the known region of working parameters, given the initial stage of characterisation. It can be seen from Fig. 8 that the ML predicted process window is wider than identified using the experimental data. This is to be expected given the wider inferences that the ML model will make using the whole training dataset. For clarity, in this figure, known failed tracks are also marked, to show that the predictions do not extend to spaces where build failures are known.

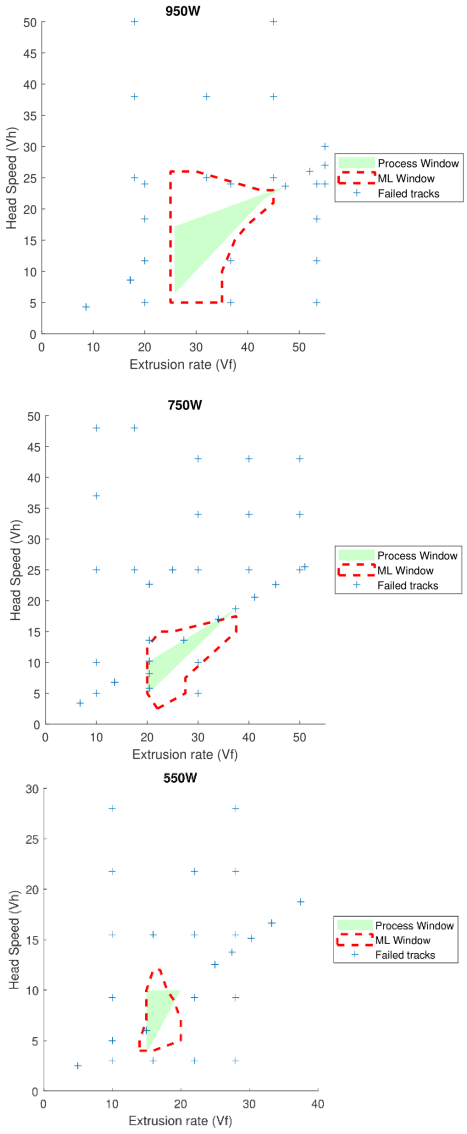

Figure 8 - Comparison of predicted and experimental process windows for good tracks

All of the ML predicted windows encompass some tracks which were measured experimentally as failed, in all cases these points had tracks which were repeated and categorised as 'Good'. These regions were drawn outside of the boundary for good parameters in the above analysis. It demonstrates the network's ability to accommodate outlying data points and the challenge of producing repeatable results in LWAM at the boundaries of the process window. Further experimental work is required to confirm this wider window. The size and accuracy of the windows is sufficiently close to support the successful predictive capability of this approach.

Fig. 9 show the measured height, width and their standard deviations for the test dataset and their correlation with the ANN's predicted values. Fig. 9 shows the points are scattered closely to the target line which represents a perfect correlation, the fit line and the R2 value for this reflects the closeness of the correlation, one indicating a perfect correlation. The results show that the models have a high accuracy for prediction of height and

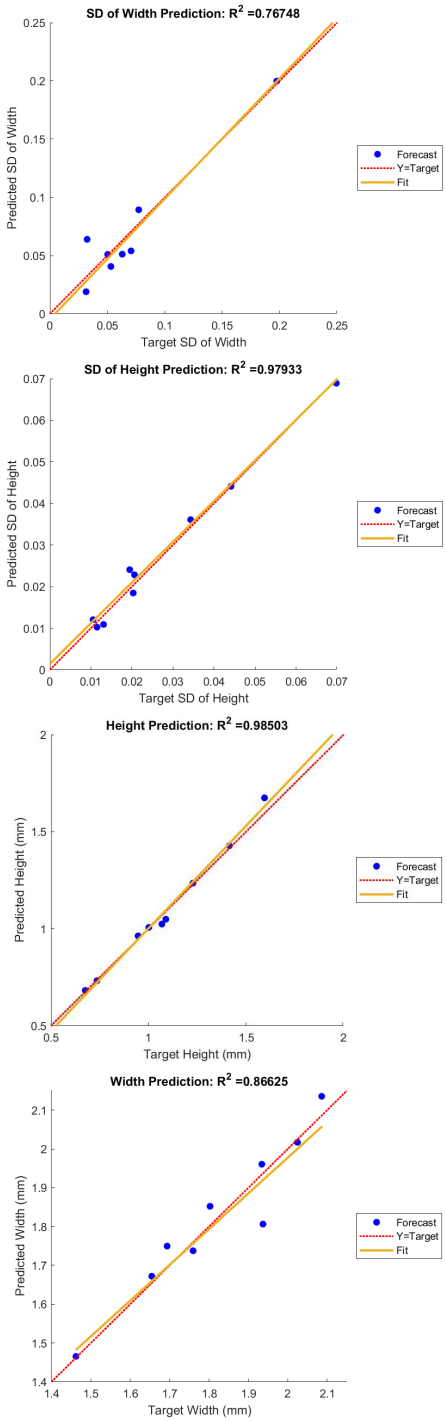

Figure 9 - Comparison of ML forecasts for Height, Width and their Standard Deviations

the standard deviation of height owing to stronger experimentally observed effects on track height. The width measurements have lower accuracy, which supports the observation from the track geometry analysis, that there was not a strong link between track width and the process parameters. The strength of the models for prediction is sufficient to support parameter planning and further refinement of process parameter for single track printing, and particularly to support identifying optimum aspect ratios for defect free track overlap [12].

IV. Conclusion and Recommendations

A method that can identify the usable range of process parameters in the form of a process window has been developed. This process produces sufficient data to train ML models in the form of two shallow Cascade Forward Neural Networks, which can effectively identify process windows and to predict basic track geometries, which have sufficient accuracy to support a subsequent parameter optimisation process.

This work has also demonstrated that track geometries produced using LWAM conform with other DED research in terms of the basic relationships between track height and width and the laser head speed and extrusion rate.

This study will be further extended to investigate whether the models and data produced can be used to support the prediction of process windows for other alloys and as a result reduce the volume and cost of experimental work required to create a similar process window.

References

1 Svetlizky, D., Das, M., Zheng, B., Vyatskikh, A.L., Bose, S., Bandyopadhyay, A., Schoenung, J.M., Lavernia, E.J., and Eliaz, N.: 'Directed energy deposition (DED) additive manufacturing: Physical characteristics, defects, challenges and applications', Materials Today, 2021

2 DebRoy, T., Mukherjee, T., Milewski, J.O., Elmer, J.W., Ribic, B., Blecher, J.J., and Zhang, W.: 'Scientific, technological and economic issues in metal printing and their solutions', Nat Mater, 2019, 18, (10), pp. 1026-1032

3 Wang, C., Tan, X.P., Tor, S.B., and Lim, C.S.: 'Machine learning in additive manufacturing: State-of-the-art and perspectives', Additive Manufacturing, 2020, 36

4 Xia, C.Y., Pan, Z.X., Polden, J., Li, H.J., Xu, Y.L., Chen, S.B., and Zhang, Y.M.: 'A review on wire arc additive manufacturing: Monitoring, control and a framework of automated system', Journal of Manufacturing Systems, 2020, 57, pp. 31-45

5 Wacker, C., Koehler, M., David, M., Aschersleben, F., Gabriel, F., Hensel, J., Dilger, K., and Droeder, K.: 'Geometry and Distortion Prediction of Multiple Layers for Wire Arc Additive Manufacturing with Artificial Neural Networks', Appl Sci-Basel, 2021, 11, (10)

6 Mozaffar, M., Paul, A., Al-Bahrani, R., Wolff, S., Choudhary, A., Agrawal, A., Ehmann, K., and Cao, J.: 'Data-driven prediction of the high-dimensional thermal history in directed energy deposition processes via recurrent neural networks', Manufacturing Letters, 2018, 18, pp. 35-39

7 Feenstra, D.R., Molotnikov, A., and Birbilis, N.: 'Utilisation of artificial neural networks to rationalise processing windows in directed energy deposition applications', Materials & Design, 2021, 198

8 Li, X., Zhang, Y., Zhao, H., Burkhart, C., Brinson, L.C., and Chen, W.: 'A Transfer Learning Approach for Microstructure Reconstruction and

Structure-property Predictions', Sci Rep, 2018, 8, (1), pp. 13461
9 Cui, W.Y., Zhang, Y.L., Zhang, X.C., Li, L., and Liou, F.: 'Metal Additive Manufacturing Parts Inspection Using Convolutional Neural Network', Appl Sci-Basel, 2020, 10, (2), pp. 545
10 Alkayem, N.F., Parida, B., and Pal, S.: 'Optimization of friction stir welding process parameters using soft computing techniques', Soft Computing, 2016, 21, (23), pp. 7083-7098
11 Caiazzo, F., Alfieri, V., Argenio, P., and Sergi, V.: 'Additive manufacturing by means of laser-aided directed metal deposition of 2024 aluminium powder: Investigation and optimization', Advances in Mechanical Engineering, 2017, 9, (8)
12 Abioye, T.E., Folkes, J., and Clare, A.T.: 'A parametric study of Inconel 625 wire laser deposition', Journal of Materials Processing Technology, 2013, 213, (12), pp. 2145-2151
13 Huang, W.H., Chen, S.J., Xiao, J., Jiang, X.Q., and Jia, Y.Z.: 'Laser wire-feed metal additive manufacturing of the Al alloy', Optics and Laser Technology, 2021, 134, pp. 106627